Nanostructured Pt-Doped Tin Oxide Films: Sol−Gel Preparation, Spectroscopic and Electrical Characterization

F. Morazzoni,*,† C. Canevali,† N. Chiodini,† C. Mari,† R. Ruffo,† R. Scotti,† L. Armelao,‡ E. Tondello,‡ L. E. Depero,§ and E. Bontempi§

Dipartimento di Scienza dei Materiali, INSTM, Università degli Studi di Milano-Bicocca, via Cozzi 53, 20125 Milano, Italy, CNR−CSSRCC, via Marzolo 1, 35100 Padova, Italy, and Laboratorio di Strutturistica Chimica, Dipartimento di Ingegneria Meccanica, Università di Brescia, Via Branze 38, 25123 Brescia, Italy

Received November 22, 2000. Revised Manuscript Received May 28, 2001

Nanostructured (3−6 nm) thin films (80 nm) of SnO_2 and Pt-doped SnO_2 were obtained by a new sol−gel route using tetra(*tert*-butoxy)tin(IV) and bis(acetylacetonato)platinum(II) as metal precursors. The results of glancing incidence X-ray diffraction (GIXRD) and X-ray photoelectron spectroscopy (XPS) investigations demonstrated that platinum substituted for tin(IV) in the cassiterite structure. Electron paramagnetic resonance (EPR) and XPS analyses showed that singly ionized paramagnetic oxygen vacancies ($V_O^\bullet$) were formed on pure SnO_2 thin films by interaction with CO atmosphere; in Pt-doped SnO_2 films, the same defects $V_O^\bullet$ fully transferred their electrons to the noble metal so that Pt(IV) became Pt(II) and Pt(0). Such samples successively exposed to air, at room temperature, reduced O_2 to O_2^-. The behavior was well-detected by EPR measurements, which showed on thin films the presence of Sn(IV)−O_2^- species. The surface reactivity agrees with the results of the electrical measurements.

Introduction

The surface reactivity of SnO_2 toward reducing and oxidizing gases is responsible for the gas-sensing properties of this semiconductor oxide. According to the currently accepted mechanisms of gas sensing, sharp increases of sensitivity are expected in the case of oxide materials having very small grain size (<6 nm).[1−4] In fact, in this case the whole SnO_2 particle is included in the space charge region and is responsible for the variation of electrical properties, typically the sensitivity S, where $S = R_{air}/R_{gas}$, and R_{air} and R_{gas} are respectively the resistance under air and under an interacting gas. The use of nanosized materials might be a powerful tool to obtain highly sensitive gas sensors. The present paper reports the preparation and the morphologic characterization by glancing incidence X-ray diffraction (GIXRD) of nanostructured SnO_2 and Pt-doped SnO_2 thin films, obtained by gelation of organometallic tin and platinum precursors.

The addition of small amounts of noble metal was commonly used to increase the sensor response.[1,5,6] Our recent studies on polycrystalline samples of transition-metal-doped SnO_2 demonstrated that the better the semiconductor−metal contact, the higher the electronic exchange at the semiconductor−gas interface.[7] When the transition metal M substituted for tin(IV) as M(IV) in the cassiterite structure, as in the case of ruthenium-doped SnO_2 powders,[8] the Schottky barrier at the metal−semiconductor contact did not ever exist and the electrons injected by CO were expected to have been completely transferred to the transition metal centers. In the case of ruthenium we demonstrated that all Ru(IV) centers were reduced to Ru(III); these in turn were able to transfer all their electrons to molecular oxygen, restoring Ru(IV) centers in SnO_2 structure. Thinking that the absence of Schottky barriers at the semiconductor−metal−oxygen interfaces is the origin of the increase in the sensitivity of the metal-doped SnO_2, we investigated here the reactivity of nanostructured (3−6 nm) platinum-doped SnO_2 in which a few Pt centers substituted for Sn(IV) centers in the SnO_2 structure. Thin films were obtained by simultaneous gelation of an alkoxide tin precursor, tetra(*tert*-butoxy)tin(IV) [Sn(OBu^t)$_4$], and a noble metal precursor, bis(acetylacetonato) platinum(II) [Pt(acac)$_2$], in the presence of acetylacetone as chemical modifier.[9−12]

* To whom correspondence should be address. Tel.: 0039 2 64485123. Fax: 0039 2 64485400. E-mail: franca.morazzoni@mater.unimib.it.
† Università degli Studi di Milano-Bicocca.
‡ CNR−CSSRCC.
§ Università di Brescia.

(1) Yamazoe, N.; Miura, N. *Chemical Sensor Technology;* Elsevier: New York, 1992; Vol. 4, pp 19−42.
(2) Xu, C.; Tamaki, J.; Miura, N.; Yamazoe, N. *J. Electrochem. Soc. Jpn.* **1990**, *58*, 1143.
(3) Xu, C.; Tamaki, J.; Miura, N.; Yamazoe, N. *Sens. Actuators, B* **1991**, *3*, 147.
(4) Ogawa, H.; Abe, A.; Nishikawa, M.; Hayakawa, S. *J. Electrochem. Soc.* **1981**, *128*, 685.
(5) Duh, J. G.; Jou, J. W.; Chiouy, B. S. *J. Electrochem. Soc.* **1989**, *136*, 2740.
(6) Matsushima, S.; Teraoka, Y.; Miura, N.; Yamazoe, N. *Jpn. J. Appl. Phys.* **1988**, *27*, 1798.
(7) Canevali, C.; Chiodini, N.; Morazzoni, F.: Scotti, R.; Bianchi, C. L. *Int. J. Inorg. Mat.* **2000**, *2*, 355−363.
(8) Canevali, C.; Chiodini, N.; Morazzoni, F: Scotti, R. *J. Mater. Chem.* **2000**, *7*, 773.

10.1021/cm001228o CCC: $20.00
Published on Web 10/09/2001

The spectroscopic investigation of both the SnO_2 defects and the chemisorbed species at the solid−gas interface are fundamental tools in understanding the gas-sensing mechanism.[13] Nanosized materials are expected to display a great increase in the amount of the spectroscopically active species, thus allowing an easier investigation of the gas−solid interaction effects. This paper reports the results of the EPR and XPS investigations performed on SnO_2 and Pt-doped SnO_2 thin films, treated with reducing (CO) or oxidizing (O_2) atmospheres in order to identify the semiconductor defects, the Pt and Sn electronic states, and the gas chemisorbed species. As for the EPR investigation, this is, to the best of our knowledge, the first time that both the paramagnetic oxygen vacancies and the paramagnetic chemisorbed O_2^- were detected on SnO_2 films without the material being scraped off the support.

Measurements of electrical resistance were also performed to determine the thin film sensitivity to CO.

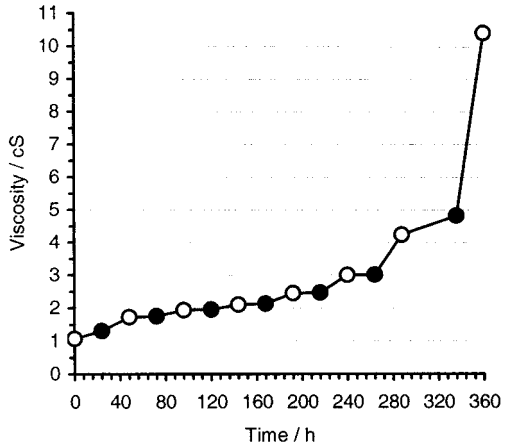

Figure 1. Plot of viscosity vs time during the addition of a hydroalcoholic solution to the ethanol solution of $[Sn(OBu^t)_4]$ and $[Pt(acac)_2]$. Full circles indicate times when the hydroalcoholic solution was added.

Experimental Section

Materials. $[Sn(OBu^t)_4]$ and SnO_2 were prepared according to ref 8. $[Pt(acac)_2]$ was an Aldrich pure reactant. Pure (argon, air, nitrogen) and mixed [CO (600 ppm)/argon], [CO (800 ppm)/air] gases were from SIAD. Films were deposited on SQ1 quartz (glass plates of 0.25 mm thickness), from SICO Jena GMBH quarzschmelze and on (100) silicon wafers (0.6 mm thick, p-type).

Preparation of SnO_2 and Pt-Doped SnO_2 Films. The sol phase was prepared by mixing, with stirring under a nitrogen atmosphere, 2.50 mL of a solution of $[Sn(OBu^t)_4]$ (360 mg/mL) in absolute anhydrous ethanol with 5.00 mL of a solution of $[Pt(acac)_2]$ (4.3 mg/mL) in ethanol−acetylacetone 1:1 v:v. After a few minutes, 1.00 mL of an ethanol−water solution, 4:1 v:v, was added and the sol phase put into a thermostatic chamber at 35 °C. After 24 h, 0.10 mL of the ethanol−water solution was added and the addition repeated every further 48 h, until the sol phase viscosity was 2.5 cS, a suitable value for the spin-coating deposition (see the next subsection). The same procedure without any $[Pt(acac)_2]$ was used to prepare the sol phase of pure SnO_2 films.

Films were deposited by the spin-coating method (spin rate 2000 rpm), dried at room temperature, and then annealed at 673 or 973 K in an air stream (50 cm^3 min^{-1}) for 2 h. At 473 K the acetylacetonate ligand was fully eliminated.[8] In the doped film the Pt:SnO_2 molar ratio was 2.5 mol %. More then one deposition (two or three) on the same substrate were sometimes performed. In this case each deposited layer was annealed in air at 673 K for 2 h before any further deposition.

The film thickness, measured by a Tencor P-10 surface profiler was 80, 160, and 240 nm for the single, double, and triple deposition.

Viscosity of the Sol Phase. Viscosity was measured with a capillary viscometer at 35 °C. The addition step by step of low amounts of hydroalcoholic solution allowed the hydrolysis and condensation rate and the consequent increase of viscosity to remain under control (Figure 1). The viscosity, measured immediately before each addition of the hydroalcoholic solution and 24 h later, slowly increased up to about 264 h (3.02 cS). Successively the increase became faster, though gelation did not occur even 360 h after the sol phase preparation (10.43 cS). The addition of the whole amount of ethanol−water solution at once hindered the good control of the hydrolysis and the condensation reaction rate. In fact, while four successive additions (0.1 mL) of the ethanol−water solution to the sol phase gave viscosity value of 2.47 cS (Figure 1), the addition at once of 0.40 mL of the ethanol−water solution to the same amount of sol phase caused the complete gelation within 24 h (the gelation time was when the sol phase lost its liquid characteristics and was transformed into a continuous phase, incorporating the total amount of solvent and holding the shape of the container).

EPR, XPS, and Electrical Measurements. EPR investigation was performed on SnO_2 and Pt-doped SnO_2 films. To have a sufficient amount of material to allow detection of the paramagnetic species, films were deposited by double deposition on both sides of 16 silica substrates (0.25 cm × 1 cm). Dried samples were annealed in an air stream (50 cm^3 min^{-1}) for 2 h at 673 K or at 973 K, then they were treated at temperatures from 298 to 673 K or from 298 to 873 K, for 30 min in CO (600 ppm)/Ar gas stream (50 cm^3 min^{-1}). Thermal annealing at temperature higher than 973 K was avoided. In the case of pure SnO_2 films, treatments with CO (600 ppm)/Ar were performed under static conditions contacting the samples at 1 atm gas pressure for 30 min. Treatments in the gas stream caused a too large dielectric loss for the EPR spectra to be recorded. After interaction with CO/Ar the films were exposed to a dry air stream (50 cm^3 min^{-1}) for 10 min at room temperature. All treatments were performed in a quartz apparatus, suitable for both gas interaction and EPR measurements. EPR spectra were recorded at 298 K directly on the films after each treatment by using a Bruker EMX spectrometer operating at the X band and magnetic field modulation of 100 kHz, with a microwave power of 100 mW and a modulation amplitude of 10 and 3 G. The g values were calculated by comparison with a DPPH standard sample (g = 2.0036). The amounts of paramagnetic species were assessed by double integration of the resonance line area, taking as the reference the area of the Bruker weak pitch ($9.7 \times 10^{12} \pm 5\%$ spin cm^{-1}).

XPS analyses were performed on samples annealed at 673 K in an air stream (50 cm^3 min^{-1}) and those successively treated in CO (600 ppm)/Ar stream (50 cm^3 min^{-1}) at 373 and at 673 K. Treatments were performed in a quartz reactor connected directly to the XPS analysis chamber to avoid contamination or surface modification of the samples due to air exposure. Spectra were recorded on a Perkin-Elmer Φ 5600-ci spectrometer using nonmonochromatized Al Kα radiation (1486.6 eV). The working pressure was $<5 \times 10^{-8}$ Pa. The standard deviation for the binding energy (BE) values was 0.15 eV. The reported BEs were corrected for the charging effects,

(9) Brinker, C. J.; Scherer, G. W. *Sol−Gel Science;* Academic Press, Inc.: San Diego, 1990; Chapter 2, pp 52−59.
(10) Sanchez, J.; Livage, M.; Henry, F.; Babonneau, *J. Non-Cryst. Solids* **1988**, *100*, 65.
(11) Chandler, C. D.; Fallon, G. D.; Koplick, A. J.; West, B. O. *Aust. J. Chem.* **1987**, *40*, 1427.
(12) Percy, M. J.; Bartlett, J. R.; Woolfrey, J. L.; Spiccia, L.; West, B. O. *J. Mater. Chem.* **1999**, *9*, 499.
(13) Iwamoto, M. *Chemical Sensor Technology*, Elsevier: New York, 1992; Vol. 4, pp 63−83.

assigning to the C1s line of adventitious carbon a value of 285 eV.[14] Survey scans were obtained in the 0−1350 eV range. Detailed scans were recorded for the C1s, O1s, Sn3d, and Pt4f regions. The atomic compositions were then evaluated by using sensitivity factors supplied by Perkin-Elmer. The chemical composition along the film thickness was evaluated by in-depth analysis. Depth profiles were carried out by Ar^+ sputtering at 2.5 keV with an argon partial pressure of 5×10^{-6} Pa. Under these conditions the sputtering rate was estimated around 10 Å min^{-1}.

To perform electrical measurements, two gold films having a rectangular shape (10 mm × 4 mm) were deposited at a distance of 2 mm from each other by a dc sputtering technique on the SnO_2 and Pt−SnO_2 thin films (10 mm × 10 mm). Such a procedure was carried out on dried films, before any thermal gas treatment. To investigate the effect of the grain size on the sensing properties, films were annealed at 673 and 973 K in a synthetic air stream (<10 nL h^{-1}) for 2 h. Electrical resistance measurements were performed in streams of air and CO (800 ppm)/air (<10 nL h^{-1}) in the temperature ranges 373−623 and 373−923 K, depending on the annealing temperature. The sensing element was equilibrated in air, then the CO/air mixture was introduced and the resistance recorded until the equilibrium conditions were reached. The initial conditions of the sensor were restored by air equilibration, before introducing again the CO mixture. Such a procedure was repeated several times.

The electrical resistance was measured by a Keithley 617 programmable electrometer connected to a PC.

GIXRD Measurements. The GIXRD (glancing incidence X-ray diffraction) data were collected by a Bruker D8 Advance diffractometer equipped with a Göbel mirror. The angular accuracy was 0.001° and the angular resolution was better than 0.01°. The Cu Kα line of a conventional X-ray source powered at 40 KV and 40 mA was used for the experiment. The XRD experimental data were analyzed using the Topas P program.[15]

Results

Microstructural Investigation. In the present study the microstructural properties of both SnO_2 and Pt-doped SnO_2 samples annealed at 673 K and at 973 K are discussed by means of glancing incidence X-ray diffraction (GIXRD) experiments.

Figure 2 shows the GIXRD spectra for all the SnO_2 and Pt-doped SnO_2 samples at an incidence angle of 1°. The peaks of samples annealed at 673 K are broader than those obtained for the samples annealed at 973 K. The profiles have been fitted and simulated with a split-PearsonVII function.[15] The average crystallite size of the films annealed at 673 K is about 3 nm, while it is about 6 nm for the samples annealed at 973 K. The sharp peaks at 52.8° and 54.5° positions are contributions of the Si substrate. To check a possible preferred orientation of the films, GIXRD measurements for different incidence angles (0.5°, 2°, 3°, 4° ,5°) were performed. Since no variation was detected in the relative intensity, the preferred orientation was excluded.

In Figure 3 the GIXRD spectrum of SnO_2 was compared with that of Pt-doped SnO_2, both annealed at 973 K. The main difference between these spectra is the intensity of the peak at 26.6° (2 Å). A similar effect was observed in the experimental spectrum of the Pt/SnO_2 film annealed at 673 K. It can be suggested that

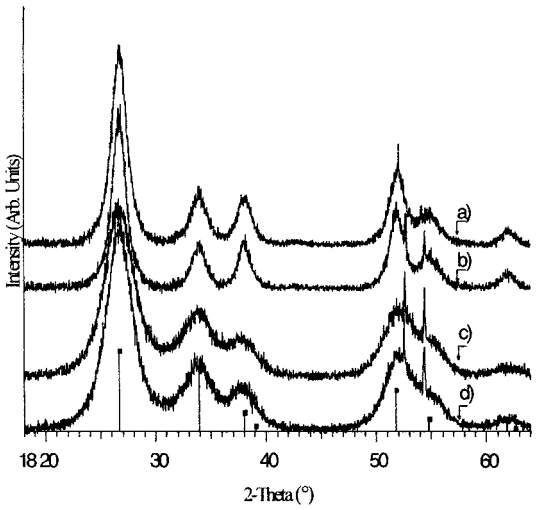

Figure 2. GIXRD spectra collected for the films of Pt-doped SnO_2 and SnO_2 annealed at 973 K (a and b, respectively) and of Pt-doped SnO_2 and SnO_2 annealed at 673 K (c and d, respectively). The incidence angle has been fixed at 1°. The reflections of the cassiterite structure are also reported as reference.

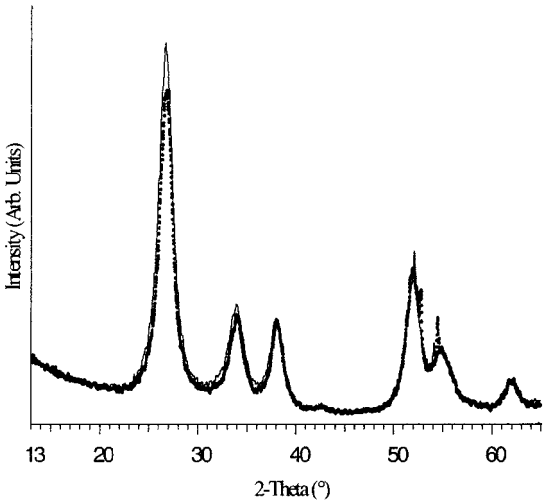

Figure 3. GIXRD spectra of Pt-doped SnO_2 (continuous curve) and SnO_2 (dotted curve) films annealed at 973 K. The main difference between these two spectra is the intensity of the peak at 26.6° (2 Å).

Pt diffuses into the SnO_2 structure, modifying the structure factors and therefore the reflection intensity of the phase. To interpret the diffraction patterns, a structural model was assumed in which Pt is substituted for Sn into the cassiterite structure. The simulation of the diffraction pattern obtained by this model, performed by the Cerius2[16] package, was in very good agreement with the experimental data and allowed us to conclude that all the dopant Pt(IV) centers substitute for Sn centers in the cassiterite lattice.

To verify possible phase segregation on the surface, the GIXRD of Pt-doped SnO_2 film annealed at 973 K was performed at the fixed incidence angles $\theta = 1°$ or 0.5°. Figure 4 showed that the spectrum at $\theta = 0.5°$ has the intensity ratio between the peaks at 52° and 54.5° reversed with respect to that observed at $\theta = 1°$. This

(14) Seah, M. P. *Practical Surface Analysis*; J. Wiley & Sons: New York, 1990; Vol. 1, p 543.

(15) Topas, P., Version 1.0.1, Bruker AXS, 1999.

(16) Cerius^2 4.0, Molecular Simulations Inc., 1999.

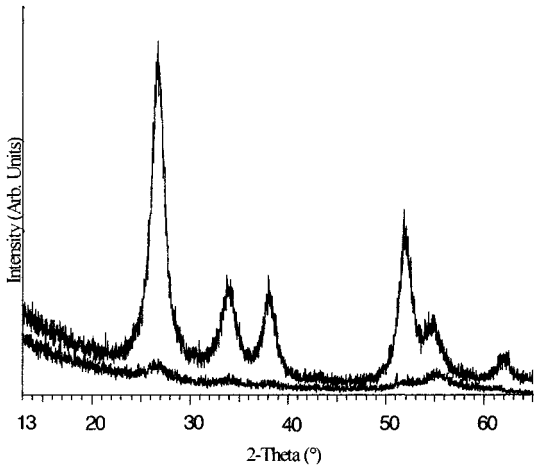

Figure 4. GIXRD spectra at different incidence angle (1°, upper curve; 0.5°, bottom curve) of Pt-doped SnO_2 films annealed at 973 K. The intensity ratio between the peaks at 52° and 54.5° (2 Å) is reversed. This effect may be due to the segregation of platinum oxide phases (see the text).

effect was absent in the spectra of Pt-doped SnO_2 films annealed at 673 K and it was attributed to the presence of an additional peak at about 55° specific to a segregated platinum oxide PtO_x phase.

Since only this reflection was detected, it was not possible to identify one particular phase. Indeed, in the range between 50° and 55° (2 Å) all the platinum oxides have strong diffraction peaks. The results of XPS investigation (see later) were indicative of the presence of PtO_2. The segregation probably took place just at the film surface, since the reflection attributed to the oxide phase was detected only by 0.5° incidence angle.

If Pt-doped SnO_2 films, previously annealed in air stream at 673 or 973 K, were treated for 30 min in CO (600 ppm)/Ar stream (50 cm^3 min^{-1}), no changes in the microstructural properties were observed in reduced samples, with respect to the oxidized ones.

XPS Investigation. XPS analyses were performed on samples annealed in air stream at 673 K (50 cm^3 min^{-1}) and subsequently treated in CO (600 ppm)/Ar stream at 373 and 673 K (50 cm^3 min^{-1}).

The binding energies (BE) values were measured for the Pt4f, Sn3d, O1s, and C1s lines and the elemental atomic percentages were calculated for undoped and Pt-doped SnO_2 films undergone different treatments. All the analyzed samples showed a single sharp component centered at 486.7 eV for the main $Sn3d_{5/2}$ spin−orbit component of the Sn3d peak, characteristic of tin oxides.[17] Another common feature to all the films was the position of the O1s signal at 530.6 eV, which is a typical value for cassiterite.[17]

In depth-XPS analysis showed that the coatings were very clear, since the C1s line, associated to adventitious carbon contamination, was merely limited to the surface region. It completely disappeared as the outer layers of the investigated samples were removed by controlled sputtering. This result confirmed that thermal annealing in air fully destroyed the acetylacetonate ligand.

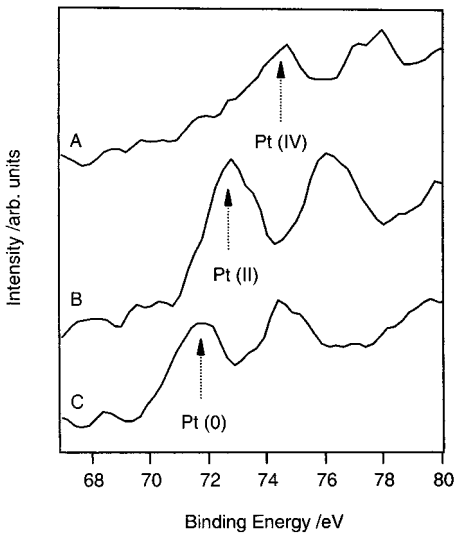

Figure 5. XPS spectrum of the Pt4f region of the Pt-doped SnO_2 film: (A) annealed in air at 673 K, (B) annealed in air at 673 K and then treated with CO (600 ppm)/Ar gas stream (50 cm^3 min^{-1}) at 373 K, (C) annealed in air at 673 K and then treated with CO (600 ppm)/Ar gas stream (50 cm^3 min^{-1}) at 673 K.

Regarding the O/Sn ratio, it resulted in lower than the expected value, i.e., 2, due to preferential sputtering of oxygen, as already observed for other oxides.[18] Concerning platinum, all Pt-doped SnO_2 films showed an homogeneous in-depth distribution of the noble metal. Variations were instead observed in the Pt4f peak position, depending on processing conditions (Figure 5). In fact, after treatment in air stream at 673 K, Pt(IV) centers (BE $Pt4f_{7/2} \cong 74.6$ eV) were detected in the outer layers of the coatings. In a different way, after treatment in CO (600 ppm)/Ar stream at 373 K, Pt(II) centers (BE $Pt4f_{7/2} \cong 72.7$ eV) were observed, whereas the treatment under reducing stream at 673 K produced platinum species (BE $Pt4f_{7/2} \cong 71.7$ eV) very close to the zero-valent state.[17]

EPR Investigation. SnO_2 and Pt-doped SnO_2 films previously annealed in air stream (50 cm^3 min^{-1}) at 673 and 973 K were investigated.

Treatments of 30 min in CO (600 ppm)/Ar (under static conditions of 1 atm pressure for pure SnO_2 or in a stream of 50 cm^3 min^{-1} for Pt-doped SnO_2 samples) were performed at temperature from 298 to 673 K or to 873 K and the EPR spectra recorded under the same atmosphere. After reduction, films were treated for 10 min in an air stream (50 cm^3 min^{-1}) and evacuated, and the spectra were recorded under argon atmosphere, to avoid line broadening due to magnetic interaction of O_2 with the surface paramagnetic species.[19]

No paramagnetic species were observed in either SnO_2 or Pt-doped SnO_2 films after air annealing at 673 and 973 K. The EPR spectrum of pure SnO_2 films after treatment with CO/Ar showed symmetrical resonance lines at $g = 1.890$, very similar to those observed in polycrystalline SnO_2 samples treated under the same reducing conditions[7,8] (Figure 6A). Signals disappeared after a 2 h air stream treatment at 673 K (50 cm^3 min^{-1}). These resonances were attributed to singly

(17) Moulder, J. F.; Stikle, W. F.; Sobol, P. E.; Bomben, K. D. *Handbook of X-ray Photoelectron Spectroscopy*; Perkin-Elmer Corp, 1992.

(18) Kelly, R. *Surf. Sci.* **1980**, *100*, 85.
(19) Che, M; Tench, A. J. *Adv. Catal.* **1983**, *32*, 1.

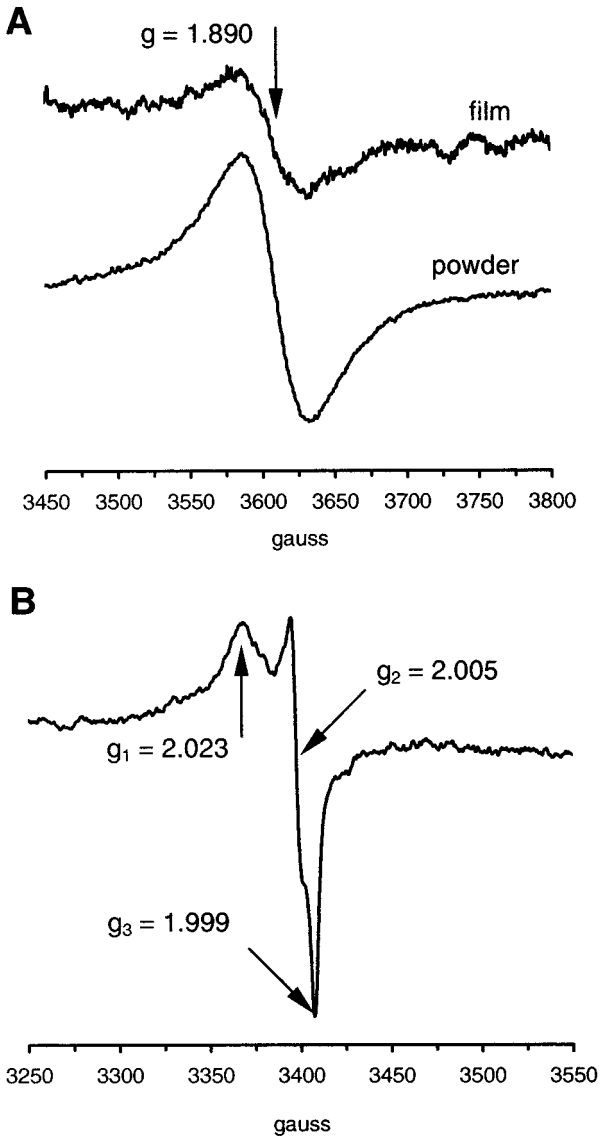

Figure 6. EPR signals of (A) $V_O^\bullet$ in SnO_2 powder and films treated with CO (600 ppm)/Ar at 673 K (1 atm under static conditions), (B) $Sn^{4+}-O_2^-$ in Pt-doped SnO_2 films treated in CO (600 ppm)/Ar stream at 673 K (50 cm^3 min^{-1}) and successively in air stream at 298 K (50 cm^3 min^{-1}).

ionized oxygen vacancies $V_O^\bullet$,[20–22] being the number of oxide lattice centers (O_O) emptied, after CO treatment, or filled, after O_2 treatment, following the reactions:

$$CO + O_O \leftrightarrow V_O + CO_2 \quad V_O \leftrightarrow V_O^\bullet + e^- \qquad (1)$$

$$V_O + {}^1/_2O_2 \leftrightarrow O_O \qquad (2)$$

V_O is a neutral oxygen vacancy, O_O an oxide anion in a regular lattice site, and e^- an electron in the conduction band. The relative amount of $V_O^\bullet$ for the 673 K air annealed films increased with the temperature of the CO treatment (Figure 7A); the order of magnitude of the absolute amount was estimated to be about 10^{14} spin g^{-1}. The intensity of the $V_O^\bullet$ signals after reduction of the films annealed in air at 973 K was comparable with the noise and did not allow a quantitative evaluation within acceptable error limits. $V_O^\bullet$ signals in pure SnO_2 films seemed unaffected by the treatment of 10 min performed in an air stream at 298 K after reduction by CO (see the Experimental Section).

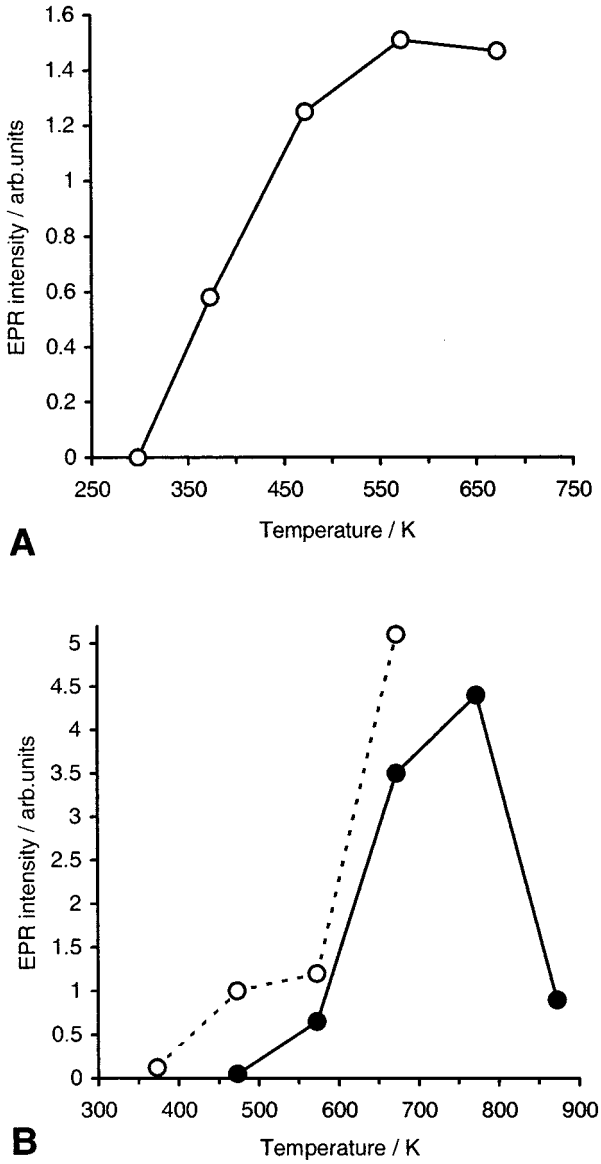

Figure 7. (A) Plot of $V_O^\bullet$ amount vs treatment temperature under CO (600 ppm)/Ar atmosphere in SnO_2 films annealed in air at 673 K; (B) $Sn^{4+}-O_2^-$ amount on Pt-doped SnO_2 films vs treatment temperature under CO (600 ppm)/Ar stream (50 cm^3 min^{-1}) and successive treatment in air stream (50 cm^3 min^{-1}) at 298 K. Open circles indicate samples annealed at 673 K in air and full circles samples annealed at 973 K.

The EPR spectrum of Pt-doped SnO_2 films did not show any resonance after CO/Ar treatment; $V_O^\bullet$ signals were completely absent. If Pt-doped SnO_2 films previously treated with CO/Ar were successively treated in an air stream at 298 K and then evacuated and put under argon atmosphere, the anisotropic resonances of the $Sn^{4+}-O_2^-$ centers ($g_1 = 2.023$, $g_2 = 2.005$, $g_3 = 1.999$)[19,20] became well-evident (Figure 6B). These were originated by the reactions

$$Sn^{4+} + O_2 + V_O^\bullet \leftrightarrow Sn^{4+}-O_2^- \qquad (3)$$

$$Sn^{4+} + O_2 + e^- \leftrightarrow Sn^{4+}-O_2^- \qquad (4)$$

$Sn^{4+}-O_2^-$ signals reversibly disappeared if the spectra

(20) Mizokawa, Y.; Nakamura, S. *Jpn. J. Appl. Phys. Supp 2, Pt 2*, **1974**, *2*, 253.

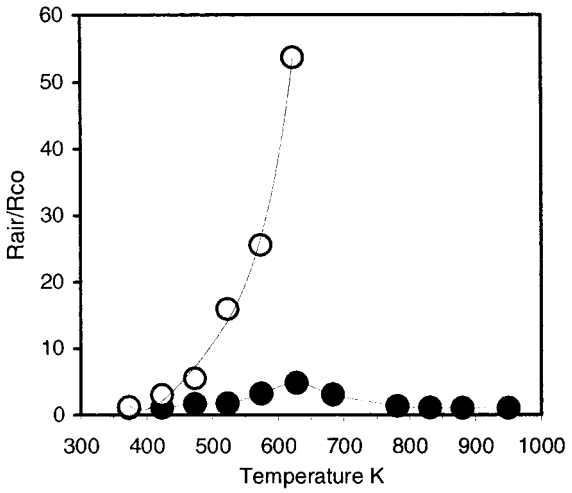

Figure 8. Plot of sensitivity (R_{air}/R_{CO}) vs temperature for Pt-doped SnO_2 films in CO (800 ppm)/Ar stream (<10 nL h^{-1}). Open circles indicate the samples annealed at 673 K in air and full circles the samples annealed at 973 K.

were recorded in air; this confirms the surface location of the superoxide species.[7,8,19] $Sn^{4+}-O_2^-$ amount increased with the CO/Ar treatment temperature, being always lower in films annealed at 973 K (Figure 7B). Pure SnO_2 films showed a very low amount of $Sn^{4+}-O_2^-$, visible when the films were reduced by CO at 773 K and successively treated in air stream at 298 K.

Electrical Properties. Pt-doped SnO_2 films treated in CO/Ar atmosphere (see Experimental Section) showed at all the temperatures electrical resistance values higher than those of pure SnO_2 films treated in a similar way.

The variation of sensitivity S with the temperature for the two different air annealed (673 and 973 K) Pt−SnO_2 films is reported in Figure 8; pure SnO_2 thin films exhibited values of sensitivity smaller than 2 in the explored temperature range. Large differences were observed in the sensing behavior of the two types of Pt−SnO_2 films. In particular, the sensitivity of the film annealed at 673 K was always increasing with the operating temperature and reaches at 623 K a value of about 9 times greater than the film annealed at 973 K. The latter instead showed a maximum shaped curve with the top value at about 623 K.

Discussion and Conclusions

The rationale for the electrical response of SnO_2 and Pt-doped SnO_2 thin films toward oxidizing and reducing atmospheres can be suggested on the basis of the results from different techniques.

EPR demonstrated that, despite the small thickness of SnO_2 films, the reduction process (1) could be assessed by direct detection and quantitative evaluation of the $V_O^\bullet$ defects on the films.

SnO_2 films were shown to be more reactive toward CO as the particle size dimension is lowered; in fact the number of EPR active $V_O^\bullet$ defects induced by the interaction with CO is higher in films annealed at 673 K, which have an average crystallite size of 3 nm, than in films annealed at 973 K, having an average size of 6 nm. This behavior agrees with the literature reports[1,13] that the crystallite size range where the particles have the highest electrical sensitivity begins from 6 nm and goes down; in this size region the whole particle reacts with the surrounding atmosphere and is fully included into the charge space region. The interaction with molecular oxygen at 298 K, following reactions 3 and 4 and detectable by EPR active $Sn^{4+}-O_2^-$, was well-visible in SnO_2 powder samples,[7,8,23] while it was always undetectable on SnO_2 films, except for a very low amount of $Sn^{4+}-O_2^-$ in films reduced by CO at 773 K. It is probable that the Schottky barrier at the film−gas interface limits the number of chemisorbed $Sn^{4+}-O_2^-$ species to EPR undetectable or very low levels. Pt-doped SnO_2 thin films did not show $V_O^\bullet$ defects under reducing conditions; on the other hand, EPR active $Sn^{4+}-O_2^-$ centers were detectable on the surface of Pt-doped SnO_2 films, after contacting with O_2 at 298 K the films reduced by CO. This is the first time, to the best of our knowledge, that chemisorbed O_2^- centers were directly detectable on thin films.

Comparing the EPR results with the results of GIXRD and XPS, we reason the following:

(i) GIXRD measurements demonstrated that Pt(IV) substituted for Sn(IV) in the lattice of the air annealed films;

(ii)XPS assessed that the reaction of Pt-doped SnO_2 films with CO reduces Pt(IV) to Pt(II) at 373 K and to Pt(0) at 673 K;

(iii)EPR revealed that no paramagnetic oxygen defects ($V_O^\bullet$) are present on the reduced Pt-doped SnO_2 films, but these films reduce O_2 to O_2^- on the surface.

These results allow us to conclude that the noble metal centers, substituting for Sn centers in the SnO_2 lattice, change their oxidation state consequently via the reaction

$$Pt^{4+} + nV_O^\bullet \leftrightarrow Pt^{(4-n)+} + nV_O^{\bullet\bullet} \quad n = 2, 4 \qquad (5)$$

All the electrons that in pure SnO_2 are constrained into the vacancies by the potential barrier were trapped by Pt^{4+} centers. Such electron trapping also agrees with the increase of electrical resistance observed for Pt-doped SnO_2 with respect to pure semiconductor SnO_2. The electrons were then transferred to oxygen following the reactions

$$Pt^{(4-n)+} + nO_2 \leftrightarrow Pt^{4+} + nO_2^- \qquad (6)$$

$$nSn^{4+} + nO_2^- \leftrightarrow nSn^{4+}-O_2^- \qquad (7)$$

It seems to us that the substitutional doped metal centers can easily transfer to oxygen the electrons accepted from the oxygen vacancies (reactions 5−7). The efficiency of the electron transfer to O_2, as it appears from the lower amount of EPR detectable $Sn^{4+}-O_2^-$ sites, decreases in films annealed at 973 K, where the crystallite size was higher and the PtO_x phase segregation was suggested. It is probable that reduced oxygen centers were formed as a consequence of reactions 6 and

(21) Kanamori, M.; Suzuki, K.; Ohia, Y.; Takahashi, Y. *Jpn. J. Appl. Phys.* **1994**, *33*, 6680.
(22) Schirmer, O. F.; Scheffler, M. *J. Phys. C: Solid State Phys.* **1982**, *15*, L 645.
(23) Canevali, C.; Chiodini, N.; Di Nola, P.; Morazzoni, F.; Scotti, R.; Bianchi, C. L. *J. Mater. Chem.* **1997**, *7*, 997.

7, but they were included into the segregated PtO_x phase, in part oxygen deficient, to fully oxidize Pt centers.

To explain why in Pt-doped SnO_2 films the number of superoxide anions observed after reduction at 873 K and air treatment at 298 K dramatically decreased (Figure 7B), it is also conceivable to suppose, on the basis of XPS results, that small Pt(0) clusters could form by the interaction with CO, mainly at the highest temperatures of reduction treatment. In this case only the Pt centers at the cluster surface may accept electrons from the oxygen vacancies.

The number of electrons transferred to O_2 by Pt-doped SnO_2, reduced at temperatures above 573 K, exceeded the double of the singly ionized vacancies observed in pure SnO_2 films (Figure 7). Assuming that the number of potentially obtainable V_O is the same as in SnO_2 films, it seems that the V_O centers generated on SnO_2 films partly transferred their electrons to Sn^{4+} centers (reaction), in analogy with the polycrystalline samples,[23] giving Sn^{2+} centers (EPR silent centers). In the presence of Pt centers, all the V_O electrons reduced Pt^{4+} centers and finally O_2.

$$n\mathrm{Sn}^{4+} + 2n\mathrm{V_O}^{\bullet} \leftrightarrow n\mathrm{Sn}^{2+} + 2n\mathrm{V_O}^{\bullet\bullet} \qquad (8)$$

Unfortunately, the XPS investigation in the valence band region could not help to distinguish Sn^{2+} from Sn^{4+} in the case of thin films as it did in polycrystalline samples.[23]

The trend of values for the electrical sensitivity of Pt-doped SnO_2 films vs temperature is very similar to that of the $Sn^{4+}-O_2^-$ amount seen by EPR in the same films (Figures 7B and 8). Thus, the electrical sensitivity seemed to be related to the possibility of transferring to oxygen the major number of the electrons stored under reductive conditions.

The maximum electrical sensitivity of the Pt-doped SnO_2 films occurred at a temperature very near that of the highest amount of $Sn^{4+}-O_2^-$ centers (Figures 7B and 8) and it is predictive of the best operating conditions for a sensor device based on this material: 673 K air annealing temperature, 623 K operative sensor temperature.

The oxoreductive mechanism suggested in reactions 5−7 lead us to conclude that the increase in the electrical SnO_2 sensitivity due to the noble metal doping could be related to the absence of the Schottky barrier at the semiconductor−gas interface in the substitutionally doped films. Interaction with CO easily reduces the noble metal centers, while interaction with O_2 reoxidized them, the number of substitutional Pt centers being the only limitation to the processes.

CM001228O